

1 **Tentative title: Modularity and selection of nectar traits in the evolution of the selfing**
2 **syndrome in *Ipomoea lacunosa* (Convolvulaceae)**
3

4 Authors: Irene T. Liao^{1,2}, Joanna L. Rifkin³, Gongyuan Cao¹, Mark D. Rausher¹

5 Addresses:
6

7 1) Department of Biology, Duke University, Durham, NC, 27708 USA

8 2) Department of Molecular, Cell, and Developmental Biology, University of California – Los Angeles, Los
9 Angeles, CA, 90095 USA

10 3) Department of Ecology and Evolutionary Biology, University of Toronto, Toronto, ON, M5S 3B2,
11 Canada
12

13 Corresponding author: Irene T. Liao, email: irene.liao@duke.edu, ireneliao@ucla.edu
14
15
16
17
18
19

20 Total word count:

21 Introduction: 957

22 Materials and Methods: 1538

23 Results: 1890

24 Discussion: 2109

25 Figures: 5 total, 4 in color

26 Tables: 3

27 Supporting Information: 7 figures, 9 methods, 1 methods and results, 9 tables
28
29
30
31
32
33
34
35

36 **SUMMARY**

37

38 • Although the evolution of the selfing syndrome often involves reductions in floral size, pollen, and
39 nectar, few studies of selfing syndrome divergence have examined nectar. We investigate whether nectar
40 traits have evolved independently of other floral size traits in the selfing syndrome, whether nectar traits
41 diverged due to drift or selection, and the extent to which quantitative trait locus (QTL) analyses predict
42 genetic correlations.

43

44 • We use F5 recombinant inbred lines (RILs) generated from a cross between *Ipomoea cordatotriloba* and *I.*
45 *lacunosa*. We calculate genetic correlations to identify evolutionary modules, test whether traits have been
46 under selection, identify QTLs, and perform correlation analyses to evaluate how well QTL properties
47 reflect the genetic correlations.

48

49 • Nectar and floral size traits form separate genetic clusters. Directional selection has acted to reduce
50 nectar traits in the selfing *I. lacunosa*. Calculations from QTL properties are consistent with observed
51 genetic correlations.

52

53 • Floral trait divergence during mating system syndrome evolution reflects independent evolution of at
54 least two evolutionary modules: nectar and floral size traits. This independence implies that adaptive
55 change in these modules requires direct selection on both floral size and nectar traits. Our study also
56 supports the expected mechanistic link between QTL properties and genetic correlations.

57

58 **KEY WORDS:** floral modularity, genetic correlations, nectar traits, phenotypic divergence, QTL, selection,
59 selfing syndrome

60

61

62

63

64

65

66

67

68

69

70

71 INTRODUCTION

72

73 Phenotypic divergence often involves changes in multiple suites of characters. Characters within a suite are
74 often developmentally or genetically integrated and form an evolutionary module, and these characters evolve
75 in a coordinated fashion (Wagner & Altenberg, 1996; Brandon, 1999; Armbruster *et al.*, 2014). By contrast,
76 divergence of different modules can be more independent. In quantitative genetic terms, traits within
77 modules evolve in a coordinated fashion because they are constrained by strong genetic correlations (Lande
78 & Arnold, 1983; Cheverud, 1984; Arnold, 1992; Armbruster *et al.*, 2014), whereas different modules evolve
79 independently because genetic correlations between modules are weak (Lewontin, 1978; Brandon, 1999). In
80 particular, adaptive change in different modules requires selection to act directly on traits of those modules.

81

82 The degree to which complex characters are composed of distinct evolutionary modules remains an
83 important question in evolutionary biology. In plants, floral traits and vegetative traits generally constitute
84 distinct evolutionary modules (Berg, 1960; Armbruster *et al.*, 1999; Juenger *et al.*, 2005; Ashman & Majetic,
85 2006; Conner *et al.*, 2014). Flowers themselves are complex structures that serve multiple functions, from
86 attracting and rewarding pollinators to promoting efficient pollen-to-ovule transfer for reproduction
87 (Armbruster *et al.*, 2004; Ordano *et al.*, 2008; Diggle, 2014). However, there is much less evidence indicating
88 whether different types of floral traits, such as flower size, nectar production, and pollen production,
89 constitute distinct evolutionary modules.

90

91 Whether flowers consist of distinct evolutionary modules is of particular importance for understanding the
92 evolution of pollination and mating system syndromes, which typically involves predictable shifts in floral size
93 and shape and nectar and pollen production (Smith, 2016; Wessinger & Hileman, 2016). This predictability
94 could arise for either of two reasons: (1) all floral traits are highly correlated genetically; or (2) flowers consist
95 of distinct evolutionary modules that undergo similar patterns of selection in different lineages. The primary
96 objective of this study is to distinguish between these explanations by asking whether nectar traits constitute
97 an evolutionary module separate from other floral traits in the evolution of the selfing syndrome.

98

99 Floral-size traits and nectar traits may not constitute distinct modules given that multiple studies have
100 demonstrated across-species correlations between aspects of flower size and nectar production (Galletto &
101 Bernardello, 2004; Stuurman *et al.*, 2004; Kaczorowski *et al.*, 2005; Galliot *et al.*, 2006; Katzer *et al.*, 2019). One
102 two-part hypothesis that could explain this correlation is that (1) both nectar volume and total sugar content
103 (the product of nectar sugar concentration and nectar volume) are proportional to nectary size; and (2)
104 genetic changes that cause smaller flowers also produce smaller nectaries by broadly affecting the cell size or
105 cell number for all floral tissues. If both criteria are true, we expect that nectar traits would not constitute a

106 separate evolutionary module distinct from floral size traits. However, if either criterion is false, then nectar
107 traits may evolve independently of floral-size traits. Because nectary size has rarely been included in studies of
108 trait divergence in pollination syndromes (but see Stuurman *et al.*, 2004; Katzer *et al.*, 2019; Edwards *et al.*,
109 2021), this hypothesis has not been evaluated for the evolution of any syndrome.

110
111 The repeated evolution of the selfing syndrome (Barrett, 2002; Arunkumar *et al.*, 2015) has fostered studies of
112 its evolution in a wide range of flowering species, including *Capsella* (Slotte *et al.*, 2012; Sas *et al.*, 2016;
113 Fujikura *et al.*, 2017; Wozniak *et al.*, 2020), *Collinsia* (Baldwin *et al.*, 2011; Strandh *et al.*, 2017; Frazee *et al.*,
114 2021), *Mimulus* (Fenster & Ritland, 1994; Fishman *et al.*, 2002, 2015), and *Ipomoea* (Duncan & Rausher, 2013b;
115 Rifkin *et al.*, 2019b, 2021). Although several studies have identified quantitative trait loci (QTLs) to assess the
116 degree to which the evolution of different syndrome traits have evolved in a correlated fashion, most have
117 focused on herkogamy, floral size, time to flowering, and pollen size and number (Rifkin *et al.*, 2021). Because
118 only one examined nectar production (nectar volume; Rifkin *et al.*, 2021), the extent to which nectar traits
119 constitute a distinct evolutionary module remains to be examined. In this study, we address this issue for a
120 pair of morning glory species, *Ipomoea cordatotriloba* and its highly selfing sister species *I. lacunosa*, which
121 exhibits the selfing syndrome.

122
123 A second issue that we address is whether reduced nectar production in the selfing *I. lacunosa* was caused by
124 selection acting directly or indirectly through correlated traits. Rifkin *et al.* (2019b) demonstrated that selection
125 was responsible for reduced nectar production in this species but could not differentiate between direct or
126 indirect selection on this trait. A finding that nectar traits constitute a distinct evolutionary module would
127 imply that much of that selection acted directly on nectar traits. Conversely, if nectar and floral dimension
128 traits constitute one evolutionary module, much of the selection to reduce nectar production may have been a
129 correlated response to selection to reduce floral size.

130
131 A third issue we address is the extent to which genetic architecture can be inferred from QTL analysis.
132 Numerous studies have identified QTLs for floral traits that differ between two species, and many have made
133 inferences about the genetic architecture of divergence based on QTL overlaps (Slotte *et al.*, 2012; Wessinger
134 *et al.*, 2014; Kostyun *et al.*, 2019). However, studies rarely evaluate the validity of these inferences. One
135 exception is Gardner and Latta (2007), whose analysis was restricted largely to crop species and within-species
136 variation.

137
138 To address these issues, we ask the following specific questions: (1) Do nectar traits constitute a separate
139 evolutionary module from floral size traits? (2) Do correlations among nectar traits support the hypothesis
140 that nectar volume and sugar content change primarily because of nectary size? (3) Did direct selection act to

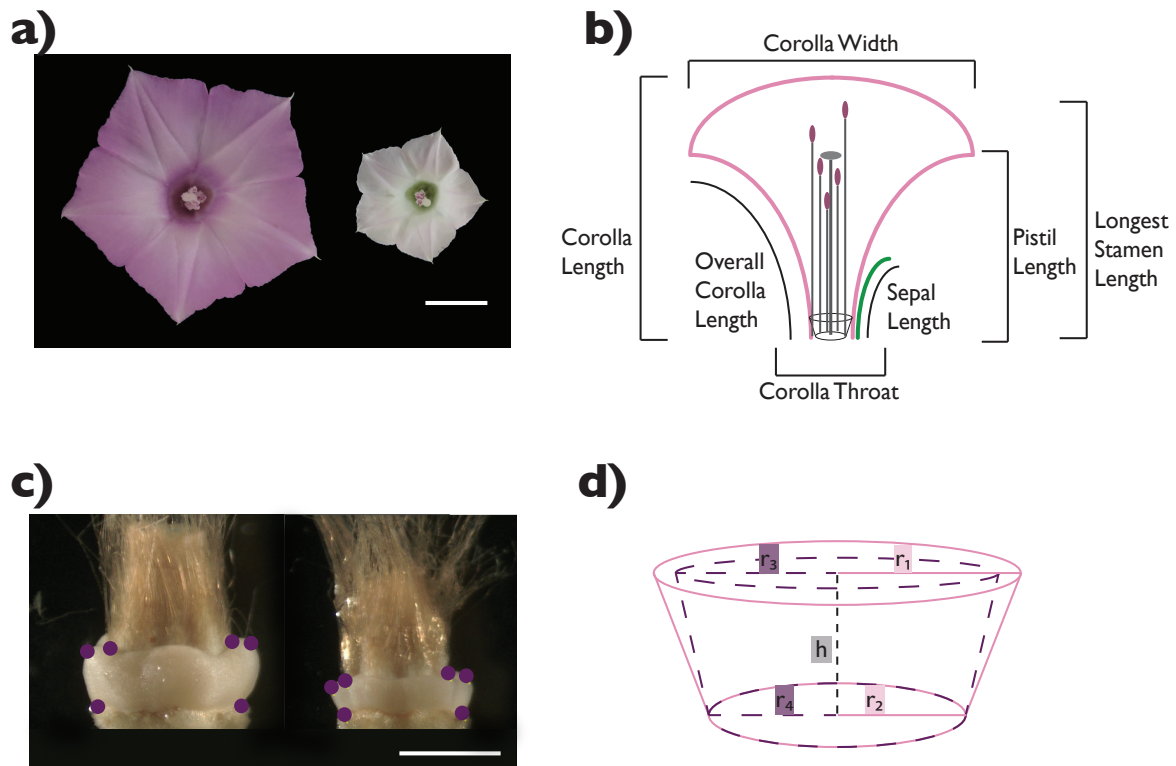
141 reduce nectar traits in *I. lacunosa*? and (4) How well do QTL properties predict the genetic architecture of
142 divergence?
143

144 MATERIALS AND METHODS

145

146 Study System

147 *Ipomoea lacunosa* L. and *Ipomoea cordatotriloba* Denn. (Convolvulaceae) are sister species in series *Batatas* (Muñoz-
148 Rodríguez *et al.*, 2018). Both are weedy species and grow widely in southeastern United States (Duncan &
149 Rausher, 2013a; Rifkin *et al.*, 2019a; USDA, NRCS, 2021). *Ipomoea lacunosa* is highly selfing (Duncan &
150 Rausher, 2013b), and compared to *I. cordatotriloba*, displays components of the selfing syndrome, including
151 reductions in overall flower size, pollen amount, pigmentation, and nectar production (McDonald *et al.*, 2011;
152 Rifkin *et al.*, 2019b; Fig. 1a).



153

154 **Fig. 0.1 Flowers and traits measured in the study**

155 a) Images of the two sister morning glory species used in the study, *Ipomoea cordatotriloba* (left) and *I. lacunosa*
156 (right). Scale bar = 1 cm. b) Floral dimension traits measured in the study. c) Image of the nectary (cream-
157 colored tissue surrounding the ovary) with purple points as landmarks for estimating the nectary size. *Ipomoea*
158 *cordatotriloba* (left) and *I. lacunosa* (right). Scale bar = 1 cm. d) Nectary size approximated as the volume of the
159 outer frustum minus the inner frustum. Formula for calculating the nectary size is as follows: $V =$
160 $\frac{\pi h}{3} [(r_1^2 + r_1 r_2 + r_2^2) - (r_3^2 + r_3 r_4 + r_4^2)]$, where h is the nectary height, r_1 is the nectary top outer radius, r_2
161 is the nectary top inner radius, r_3 is the nectary bottom outer radius, and r_4 is the nectary bottom inner radius.

162

163 **Materials and growing conditions**

164 One *I. cordatotriloba* individual was crossed by one *I. lacunosa* individual to generate F1 hybrids (Duncan &
165 Rausher, 2013b; Rifkin *et al.*, 2021). One F1 (CL5) was selfed to generate a mapping population of 500 F2s;
166 these were selfed by single seed decent for 3 more generations to generate 322 recombinant inbred lines
167 (RILs) at the F5 generation. Two individuals per RIL and 24-25 selfed offspring of each parent were selected
168 for genotyping and phenotyping.

169

170 Scarified seeds were planted directly into soil in 24-cell seed packs in randomized positions and grown under
171 12-hour light:12-hour dark at 21-23°C to induce floral bud formation. After a month, the plants were
172 transferred to the Duke University Greenhouses and grown under the following conditions: 12-hour light:12-
173 hour dark, light temperatures 23-26°C, dark temperatures 16-19°C.

174

175 **F5 Phenotyping**

176 Prior to planting, three seed traits – length, width, and mass – were measured using calipers and a balance
177 sensitive to 0.001 grams. Seven flower-size traits were measured on open flowers using a digital caliper
178 (“Mitutoyo Digimatic CD6" CS): corolla width, corolla throat, corolla length, overall corolla length, sepal
179 length, longest stamen length, pistil length (Fig. 1b). Three nectar-related traits were measured: nectar volume,
180 nectar sugar concentration, and nectary size. For 675 out of 686 total individuals, floral and nectar traits were
181 measured on at least three flowers per individual plant.

182

183 Methods for measuring nectar volume and sugar concentration are detailed in Rifkin *et al.* (2019a) (Methods
184 S1). Flower buds were capped the day before flower opening to limit nectar evaporation. Nectar was collected
185 using 2µl microcapillary tubes (Drummond Scientific), and the height of the liquid in the tubes was measured
186 with a caliper to determine nectar volume. All nectar was expelled onto a Master-53M ATAGO refractometer
187 to measure sugar concentration. Nectaries were photographed and images were measured by selecting six
188 points to designate the outline of the nectary (Fig. 1c). The distance between sets of points was calculated to
189 obtain the variables to estimate the nectary size, which is modeled after the volume of a frustrum (Fig. 1d).

190

191 **Genotyping and sequencing data**

192 Most phenotyped individuals were also genotyped (Table S1). DNA was extracted using the GeneJET
193 ThermoFisher Plant Genomic DNA Purification Kit (Thermo Fisher Scientific). We used a modified double-
194 digest restriction assisted DNA (ddRAD) library preparation protocol (Peterson *et al.*, 2012) combined with
195 the Rieseberg lab genotype-by-sequencing protocol (Ostevik, 2016; Methods S2). All samples were pooled in
196 equal amounts (100 ng) before sequencing over 4 lanes of the Illumina HiSeq 4000 platform (150bp PE

197 reads) at the Duke Center for Genomic and Computational Biology Sequencing and Genomic Technologies
198 Core. Raw sequence data are deposited in the NCBI Sequence Read Archive [accession: PRJNA732507].

199

200 **Sequence processing and genetic map**

201 Markers determined from ddRAD sequencing reads were aligned to the draft *I. lacunosa* genome using
202 NextGenMap (Sedlazeck *et al.*, 2013), and a linkage map for F5 individuals was constructed concurrently with
203 F2 individuals (Rifkin *et al.*, 2021) using Lep-Map3 (Rastas, 2017; Methods S3). This process resulted in a total
204 of 6056 markers with 174-625 markers per linkage group (Supporting Information Fig. S1). A “consensus”
205 genotype was found at each position for each RIL by comparing the genotypes between the two individuals;
206 if the genotypes were the same, the genotype was kept. All other scenarios were coded as missing data.
207 Overall, there was 11% missing genotype data.

208

209 **Summary statistics**

210 The final dataset includes a total of 635 individuals phenotyped: 313 lines where both replicates were
211 phenotyped; 9 lines where only one individual was phenotyped; 624 individuals where at least three flowers
212 were phenotyped and 11 individuals where only one or two flowers were measured. Summary statistics were
213 calculated in R version 4.0.2 (R Core Team, 2020).

214

215 **Correlations & heritabilities**

216 Genetic correlations were calculated for all traits on F5 RILs in two ways: (1) as the correlation of line means,
217 and (2) from variance and covariance components in a Multivariate Analysis of Variance, in which line is the
218 main effect (Falconer & Mackay, 1996; Methods S4). Because these correlations are calculated from inbred
219 lines, they represent broad-sense genetic correlations. Broad-sense heritabilities were calculated for each trait
220 in a similar fashion (Methods S4).

221

222 **Cluster analysis**

223 We used cluster analysis to identify evolutionary modules using three algorithms: Complete, Ward, and
224 McQuitty with the function *hclust* (Müllner, 2013) in R. All gave similar results (Fig. S2). We computed the
225 average and standard error of pairwise trait genetic correlations within and between each module. As an
226 indication of whether the identified modules are real, we performed a permutation test (Methods S5).

227

228 **QTL analysis**

229 QTL analyses were performed using both *qtl* (Broman *et al.*, 2003) and *qtl2* (Broman *et al.*, 2019) with the
230 consensus genotypes and the average phenotypic values for each RIL. Most traits were approximately

231 normally distributed, except for seed mass, seed width, nectar volume, and nectary size, which have slightly
232 skewed distributions (Fig. S3).

233

234 We first used *qtl2* to identify QTLs using the `scan1` function with a linear mixed model leave-one-
235 chromosome-out (LOCO) method (Yang *et al.*, 2014; Broman *et al.*, 2019) with genome-wide LOD
236 significance thresholds ($\alpha=0.05$, 1,000 permutations) and chromosome-wide LOD significance thresholds
237 ($\alpha=0.05$, 10,000 permutations). We then used a multiple QTL mapping approach in *qtl* with the Haley-Knott
238 regression method to determine non-spurious QTLs using the `scantwo` function to determine the penalties at
239 $\alpha=0.05$ to use in the `stepwiseqtl` function. We started the multiple QTL model selection with genome-wide
240 significant QTLs identified with the LOCO method, searching for only for additive QTLs. Confidence
241 intervals were estimated at 1.5-LOD intervals.

242

243 We created two QTL datasets from these approaches. The first (designated “GWS QTL”) combined the
244 QTLs significant genome-wide from the LOCO method and from the multiple QTL model. The second
245 dataset (“ALL QTLs”) included all QTLs significant at the chromosome-wide thresholds, including multiple
246 QTL peaks within a chromosome and most GWS QTLs, from the LOCO method.

247

248 We calculated the relative homozygous effect (RHE) as the difference between the mean trait values of
249 homozygotes at the trait QTL peak divided by the difference between the mean trait values of the two
250 original parents. Summing the RHE values for a trait provides an indication of the completeness of QTL
251 discovery: A value substantially less than 1.0 indicates that a substantial number of QTLs have not been
252 detected, whereas a value near 1.0 suggests most QTLs affecting a trait have been identified.

253

254 Downstream analyses were performed separately for both the GWS QTL and ALL QTL datasets. We
255 evaluate which dataset provides a better explanation of genetic architecture by assessing how well they explain
256 genetic correlation patterns.

257

258 **Predicting genetic architecture from QTL properties**

259 Genetic correlations provide the best estimate of genetic architecture because they include the effects of all
260 QTLs influencing a trait. Using properties of detected QTLs to infer genetic architecture is likely to be less
261 reliable because typically not all QTLs affecting a trait are identified in QTL studies. To determine how well
262 the genetic architecture of divergence is predicted by QTL properties, we examined properties of QTL co-
263 localization. We considered QTLs for two traits to co-localize if their 1.5-LOD confidence intervals
264 overlapped (Slotte *et al.*, 2012; Wessinger *et al.*, 2014; Kostyun *et al.*, 2019). To determine whether the overall
265 degree of overlap was greater than expected by chance, we performed a randomization test (Methods S6). We

266 quantified the degree of QTL overlap between two traits, examined whether QTL overlap could explain the
267 observed modularity, and determined whether there was greater overlap within modules than between
268 modules using a permutation test. We also assessed how well QTL overlap explained the observed genetic
269 correlations (Methods S7).

270

271 We calculated a “predicted” genetic correlation from QTL properties, r_Q , using a modification of the
272 approach presented in Gardner and Latta (2007) (Methods S8). We assessed how well r_Q matched the
273 estimated true genetic correlations (r_G) by the correlation between r_Q and r_G . We also calculated the correlation
274 between average total RHE for a trait pair and bias ($r_Q - r_G$) (Gardner & Latta, 2007). To determine the
275 significance of these correlations, we performed a permutation analysis (Methods S8). Finally, we determined
276 whether bias involving floral and nectar traits differed for the two QTL sets by bootstrapping (1,000
277 replicates).

278

279 **Analyses of selection**

280 To test for whether selection contributed to the divergence of the 13 traits, we used the ν test from Fraser,
281 2020 (Methods S9) and the QTL-EE sign test (Orr, 1998). Because the QTL-EE test cannot detect selection
282 if there are fewer than eight QTLs for a trait (Fraser, 2020), we applied this test only to traits with eight or
283 more QTLs. Additionally, we performed simulations to evaluate the extent to which ascertainment bias might
284 contribute to an increased false discovery rate (Results and Methods S1, Anderson & Slatkin, 2003).

285

286 **RESULTS**

287

288 **Phenotypic differences**

289 Trait differences between parent individuals, as measured on their selfed offspring, were consistent with a
290 previous study (Rifkin *et al.*, 2019b) showing that *I. lacunosa* and *I. cordatotriloba* differ in multiple flower size
291 and nectar traits (all traits differ significantly, $P < 0.05$ after correcting for multiple hypotheses (Benjamini &
292 Hochberg, 1995; Table 1). Of the traits not examined previously, nectary size was smaller, and seed mass,
293 seed width, and seed length were larger in the selfing *I. lacunosa* compared to the mixed-mating *I. cordatotriloba*.

294 **Table 0.1 Summary of means and standard errors of 13 traits.**

295 Means and standard errors were calculated for *Ipomoea cordatotriloba* (n=25; 24 selfed offspring, 1 parent) and *I.*
 296 *lacunosa* (n=26; 25 selfed offspring, 1 parent) and F5 RILs (F5, n = 322). All traits are significantly different (P
 297 < 0.05) from a t-test and corrected for multiple hypotheses testing (Benjamini & Hochberg, 1995). Asterisks
 298 indicate the traits (all seeds) that do not include the parents in the mean and standard error calculations.
 299

Category	Trait	Units	<i>Ipomoea cordatotriloba</i>	F5 hybrids	<i>Ipomoea lacunosa</i>
Seed	Seed Length*	mm	4.194 (0.0378)	4.416 (0.0182)	4.621 (0.036)
Seed	Seed Mass*	g	0.0242 (0.000678)	0.0285 (0.000236)	0.0292 (0.000555)
Seed	Seed Width*	mm	3.836 (0.0383)	4.016 (0.0142)	4.156 (0.0322)
Nectar	Nectar Sugar Concentration	mg/mL	382.845 (2.729)	311.498 (1.75)	247.743 (6.474)
Nectar	Nectar Volume	μl	3.239 (0.131)	1.55 (0.0301)	0.517 (0.0445)
Nectar	Nectary Size	mm ³	0.186 (0.0077)	0.102 (0.0016)	0.058 (0.00251)
Flower size	Sepal Length	mm	11.539 (0.0965)	11.085 (0.0432)	10.876 (0.137)
Flower size	Corolla Width	mm	28.101 (0.288)	21.858 (0.107)	16.424 (0.263)
Flower size	Corolla Throat	mm	7.446 (0.0769)	6.509 (0.0267)	5.588 (0.0667)
Flower size	Pistil Length	mm	16.025 (0.163)	13.945 (0.0758)	10.748 (0.145)
Flower size	Longest Stamen Length	mm	19.418 (0.111)	15.954 (0.0653)	12.467 (0.114)
Flower size	Corolla Length	mm	26.606 (0.198)	22.566 (0.0906)	17.526 (0.214)
Flower size	Overall Corolla Length	mm	32.357 (0.244)	26.573 (0.106)	20.066 (0.277)

300

301 **Nectar traits**

302 Nectar volume (NV) and total sugar amount (TS) are highly correlated ($r = 0.98$; Fig. S4b,c). Both nectar
 303 volume and total sugar amount also exhibit significantly non-linear relationships with nectary size, with both
 304 regressions having high R^2 values (~ 0.92), indicating that the regressions account for much of the variation
 305 seen in nectar volume and total sugar amount (Fig. S4e,f). From these regressions, we derived a relationship
 306 that predicted sugar concentration (NSC) as a function of nectary size (NS): $NSC(NS) = TS(NS)/NV(NS)$.
 307 This predicted relationship is very similar to the relationship between measured sugar concentration and
 308 nectary size (Fig. S4g). Because total sugar amount is a derived value with a nearly exact correspondence with
 309 nectar volume, we do not include total sugar amount in subsequent analyses.

310

311 **Genetic correlations and evolutionary modules**

312 Genetic correlations calculated from the variance-covariance components are similar to those calculated from
 313 the RIL means ($r = 0.981$, $p < 0.05$, Fig. S5). We thus used only the former in subsequent analyses.

314

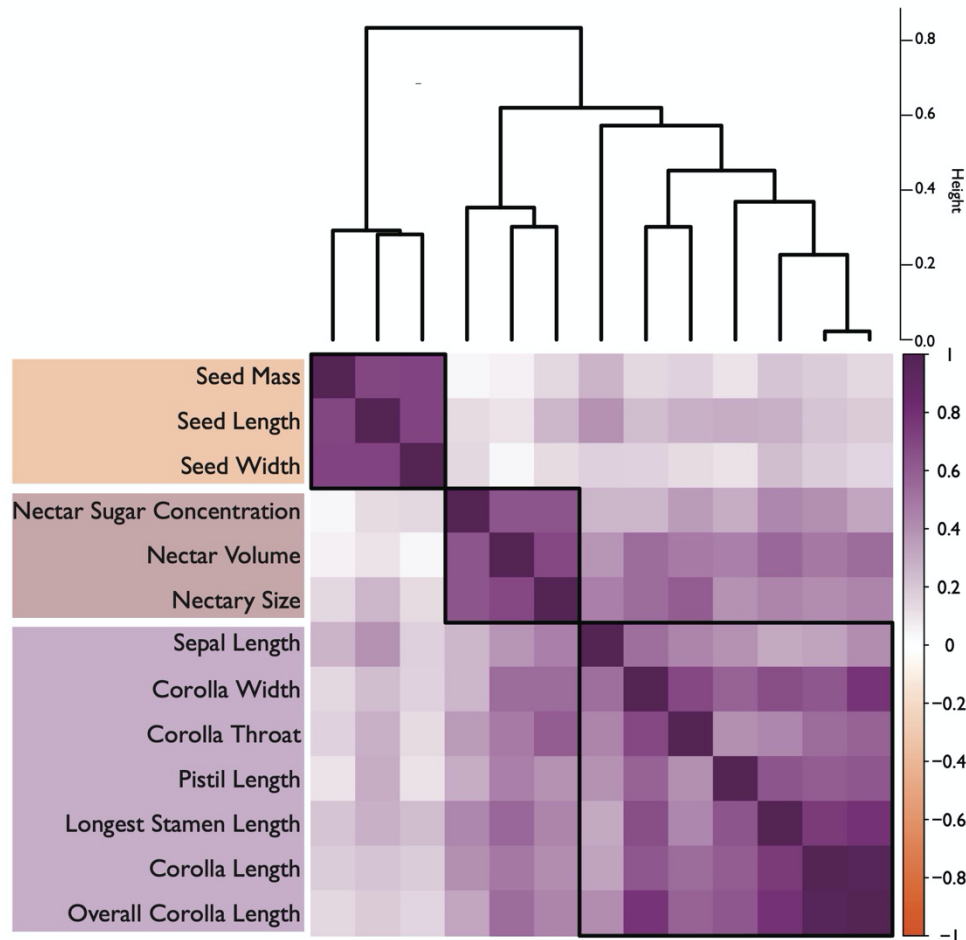
315 Pairwise genetic correlations are positive for all traits, as are most pairwise environmental correlations (Table
 316 S2, Fig. S6b,c). The three clustering algorithms produced similar results: The 13 traits form three distinct

317 clusters, which we interpret as evolutionary modules. The “flower module” consists of all floral size traits, the
318 “nectar module” consists of the three nectar traits, and the “seed module” consists of the three seed-size
319 traits (Fig. 2, S2). The average correlations within each module are substantially higher (range 0.557-0.656)
320 than the average correlations between traits in different modules (range 0.008 – 0.226; Table 2a). The average
321 within-module correlation (0.602) is more than 5 times the average between-module correlation (0.117)
322 (Table 2a).

323

324 Generally, this pattern suggests that evolution of the three modules has been largely genetically independent.
325 Nevertheless, a moderate average genetic correlation (0.226) exists between floral and nectar traits (Table 2a),
326 suggesting that there may have been some correlated evolution of these two modules.

327



328

329 **Fig. 2 Cluster diagram and heatmap based on variance-covariance-component genetic correlations.**

330 Cluster dendrogram portrayed for the “mcquitty” method. Boxes in the heat map indicate the three clusters.

331 Other clustering methods result in the same three clusters (Fig. S6). For the heatmap, strong positive

332 correlations are in dark purple while weak to no correlation range from light purple to white. (left to right)

333 seed, nectar, and flower size. Pairwise genetic correlation values are found in Table S1.

334

335 A permutation test that randomly assigned the observed correlations to trait pairs indicated that the modules
 336 identified reflect groups with correlations that are higher than expected by chance. In 1,000 permutations, no
 337 values of the difference between average correlations within and between modules was as large as the
 338 observed difference of 0.485, allowing rejection of the null hypothesis at $P < 0.001$.

339

340 **Table 0.2 Average genetic correlations and QTL overlap within and between modules.**

341 a) Average genetic correlations calculated from variance and covariance components. Average within- and
 342 between-module correlations are 0.602 and 0.117, respectively. Permutation test of hypothesis that within-
 343 module correlations do not differ from between-module correlations: $P < 0.001$. b) Average QTL overlap for
 344 GWS QTLs. Average within- and between-module correlations are 0.248 and 0.086, respectively. Permutation
 345 test of hypothesis that within-module correlations do not differ from between-module correlations: $P =$
 346 0.078. c) Average QTL overlap for ALL QTLs. Average within- and between-module correlations are 0.464
 347 and 0.275, respectively. Permutation test of hypothesis that within-module correlations do not differ from
 348 between-module correlations: $P = 0.047$.

349

a) GENETIC CORRELATIONS

MODULE	seed	nectar	flower
seed	0.651 (0.0655)	0.117 (0.0224)	0.0077 (0.0087)
nectar	0.117 (0.0224)	0.557 (0.1189)	0.226 (0.0177)
flower	0.0077 (0.0087)	0.226 (0.0177)	0.601 (0.0381)

b) QTL OVERLAP – GWS QTLs

MODULE	seed	nectar	flower
seed	0.111 (0.111)	0.041 (0.023)	0.080 (0.015)
nectar	0.041 (0.023)	0.112 (0.082)	0.110 (0.014)
flower	0.080 (0.015)	0.110 (0.014)	0.286 (0.031)

c) QTL OVERLAP – ALL QTLs

MODULE	seed	nectar	flower
seed	0.460 (0.111)	0.216 (0.049)	0.214 (0.031)
nectar	0.216 (0.049)	0.500 (0.096)	0.360 (0.024)
flower	0.214 (0.031)	0.360 (0.024)	0.459 (0.028)

350

351

352

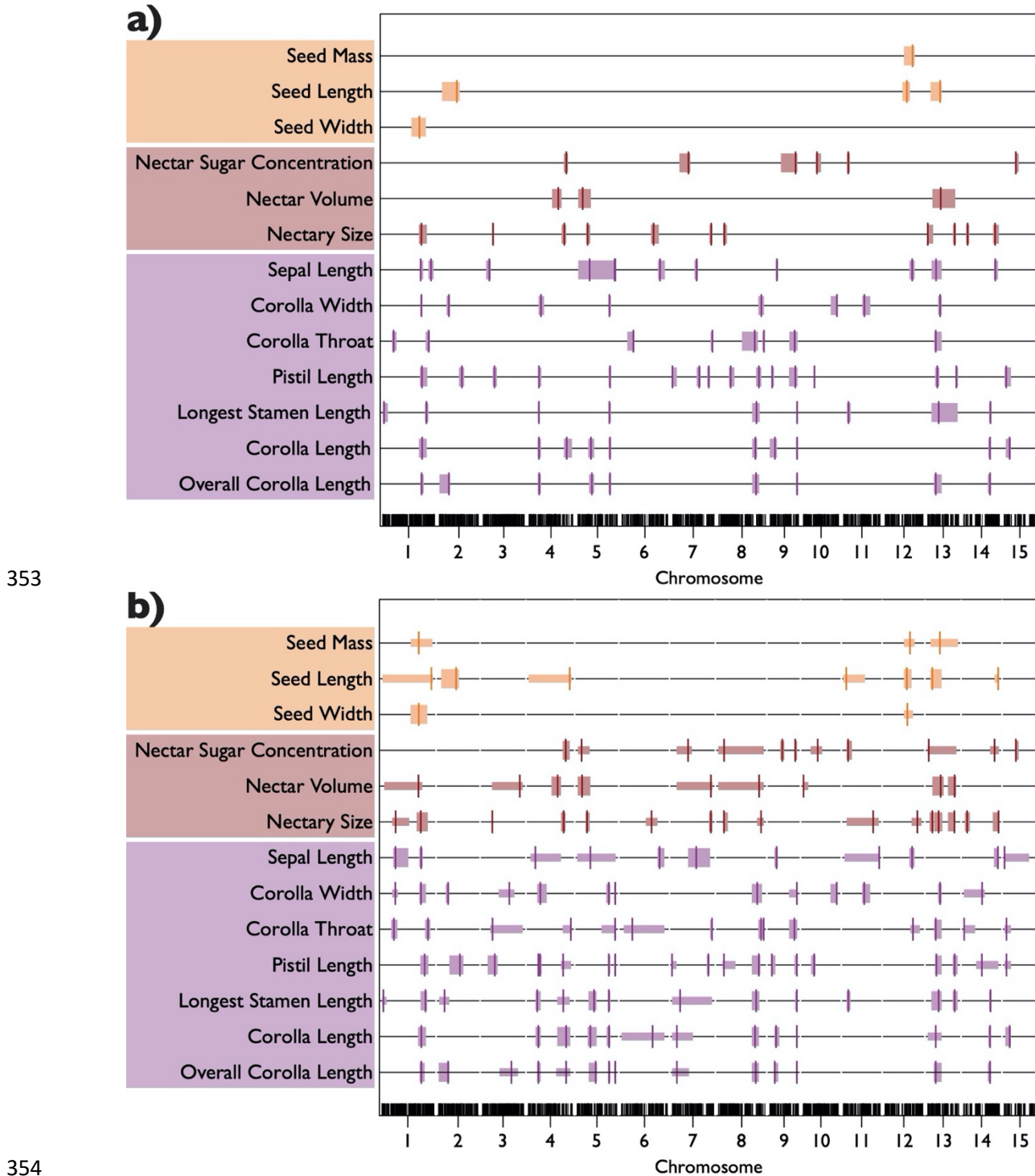


Fig.3: Chromosome map of QTLs for 13 phenotypic traits.

Each bar represents the 1.5 LOD confidence interval with the vertical line indicating the QTL peak. Bars in orange hues represent seed traits; maroon red hues represent nectar traits; purple hues represent flower traits. A summary of QTL peaks is found in Table S2. Individual trait QTL plots are found in Fig. S7. a) Genome-wide significant (GWS) QTLs – combination of the two most stringent QTL models. b) ALL QTLs – based on multiple QTL peaks from the LOCO method. Thicker bars indicate peaks significant at the genome-wide threshold; thinner bars indicate peaks significant only at the chromosome-wide threshold.

362 **QTL analyses: number and effect sizes**

363 Combining QTLs with genome-wide significance from the LOCO model and the multiple QTL model (GWS
364 QTLs), we identified 97 QTLs. From just the LOCO model with chromosome-wide significance (CWS),
365 ALL QTLs produced total of 146 QTLs (92 GWS and 54 CWS; Fig. 3, S7, Table S3). QTLs were located
366 throughout the genome, with 3-12 QTLs per chromosome for GWS QTLs and 4-17 QTLs for ALL QTLs.
367 Most traits have more than 5 QTLs detected, except for seed mass and seed width (in both QTL datasets)
368 and nectar volume and seed length (in GWS QTLs).

369

370 Most QTLs are of small to moderate effect (Table S3, S4). For GWS QTLs, mean RHE for most traits was
371 less than 0.15, except for seed mass (0.375) and seed width (-0.372). The maximum RHE was less than 0.25
372 for nine traits and was less than 0.5 for the three seed traits. Only sepal length had a large-effect QTL (RHE
373 = 0.891). The pattern was similar for ALL QTLs: all traits had a mean RHE less than 0.15 in absolute value,
374 nine traits had a maximum RHE less than 0.25, and seed traits had a maximum RHE less than 0.5.

375

376 For floral traits, total RHE values are relatively high (GWS QTLs: 0.461 – 1.134, mean = 0.802; ALL QTLs:
377 0.721 – 1.562, mean = 1.013), suggesting that the identified QTLs account for much of the difference
378 between the two species (Table S3b). Less is accounted for by nectar traits (GWS QTLs: 0.247 – 0.654, mean
379 = 0.436; ALL QTLs: 0.563 – 0.904, mean = 0.740), indicating the existence of an unknown number of
380 undetected QTLs. Finally, we were least successful in recovering QTLs for seed traits (GWS QTLs: -0.372 –
381 0.375, mean = 0.078; ALL QTLs: less than 0).

382

383 **QTL overlap and genetic correlations**

384 The pattern of average QTL overlap is similar to that exhibited by genetic correlations (Table 2). For both
385 QTL sets, the average within-module QTL overlap was greater than that between modules (Table 2b,c).
386 However, comparisons with genetic correlations differ somewhat for the two datasets. For GWS QTLs, the
387 within-module QTL overlap averages are lower than, while the between-module QTL averages are similar to,
388 the corresponding genetic correlation averages (Table 2a,b). By contrast, for ALL QTLs, the within-module
389 overlap averages are more similar to the corresponding genetic correlation averages (Table 2a,c), while the
390 between-module averages are somewhat higher. The within- and between-module averages of the predicted
391 genetic correlations, r_Q , also show similar patterns when compared to the actual genetic correlations (Table 2,
392 S6).

393

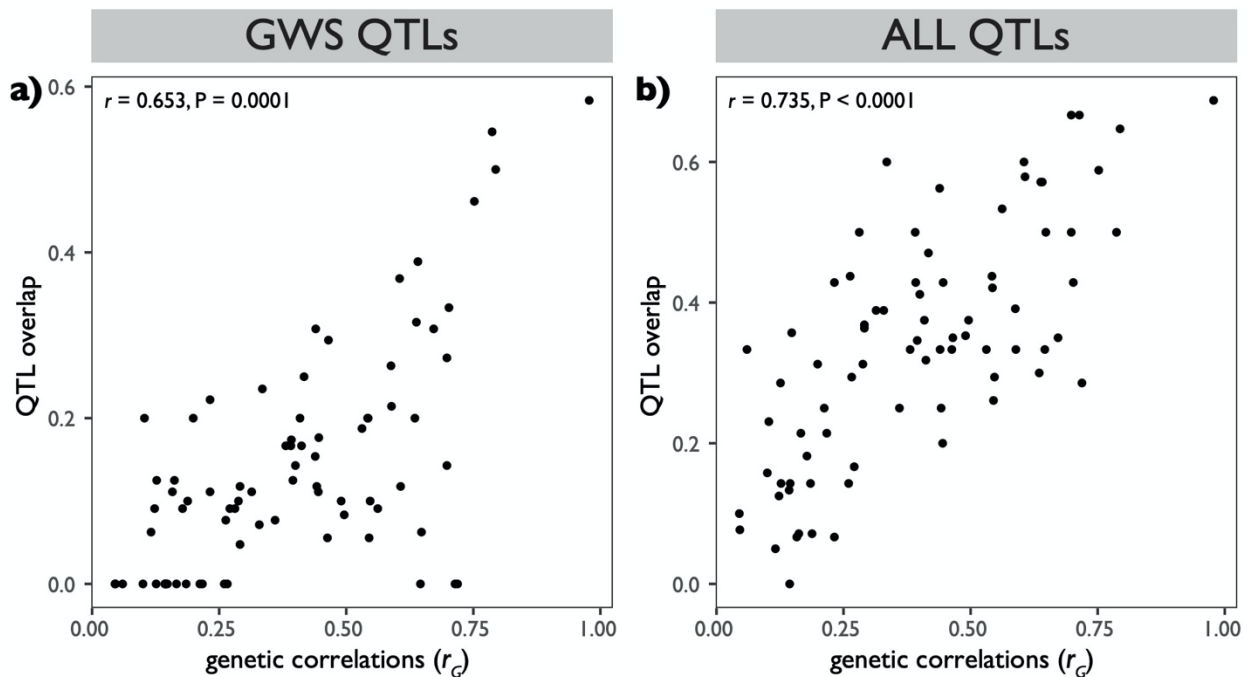
394 The randomization test, in which we assigned each QTL to a random position in the genome and calculated
395 the resulting QTL overlap (Table S7), indicated that there is greater overlap among QTLs within modules
396 than would be expected by chance. For GWS QTLs, this test was significant ($P < 0.0001$) across all modules

397 combined. However, this result is likely primarily due to overlap found within the floral-size module ($P <$
398 0.0001; Table S7a); neither the nectar nor the seed modules differ from the null hypothesis of random
399 placement of QTLs in the genome (Table S7a). By contrast, for ALL QTLs the test is significant both over all
400 the modules combined and for each module individually (Table S7b). These results are consistent with
401 within-module pleiotropy of QTLs.

402

403 For individual trait pairs, rather than the module averages considered above, QTL overlap and the predicted
404 genetic correlations, r_G , are generally reflective of the magnitude of the corresponding genetic correlations, r_G ,
405 for both GWS and ALL QTLs. The correlation between r_G and the QTL overlap is significant for both GWS
406 QTLs and ALL QTLs (Fig. 4), as is the correlation between r_G and r_Q (Fig. 5a). A subset of r_Q values is
407 negative and correspond largely to pairwise correlations that include at least one seed trait. Omitting seed
408 traits, the correlation between r_G and r_Q is reduced somewhat for both QTL sets but remain highly significant
409 (Fig. 5b). These patterns suggest that the magnitude of QTL overlap and the predicted genetic correlations
410 capture the actual genetic correlation between traits reasonably well.

411



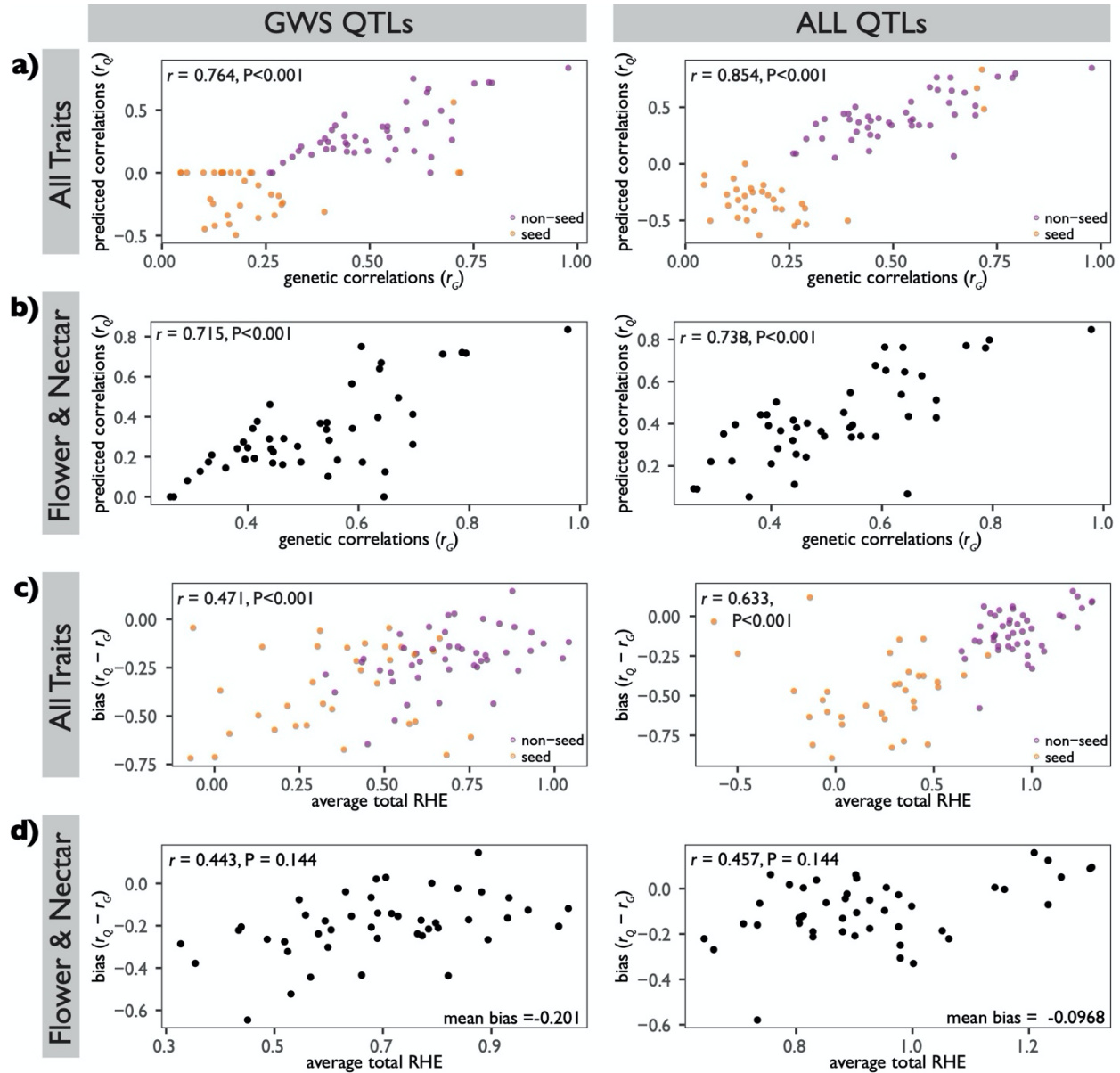
412

413 **Fig. 4 Comparison of genetic architecture based on genetic correlations versus QTL overlap.**

414 Figures portray correlation between genetic correlations and QTL overlap for all trait pairs. a) QTL overlaps
415 based on GWS QTLs only. b) QTL overlaps based on ALL QTLs.

416

417



418

419 **Fig.5 Accuracy of predicted correlations.**

420 The average total RHE was calculated by taking the average of total RHE for the two traits. Significance of
 421 correlation was determined by a permutation test. a) Correlation between r_G and predicted genetic
 422 correlations from QTL effects (r_Q) for all traits. b) Same as a) but excluding seed traits. c) Correlation
 423 between bias and average total RHE for all traits. d) Same as c) but excluding seed traits. For a) and c),
 424 orange points indicate correlations that include one of the seed traits; purple points indicate correlations of
 425 non-seed traits (floral and nectar traits only). For all figures, comparisons for GWS QTLs are on the left;
 426 those for ALL QTLs are on the right.

427

428

429 The accuracy of the predicted genetic correlation is reflected in the bias, $r_Q - r_G$. For both GWS QTLs and

430 ALL QTLs, bias was significantly less for trait pairs with greater total RHE (Fig. 5c). Although this pattern

431 holds after removing the correlations that include seed traits, the permutation test is not significant for either

432 QTL set (Fig. 5d). For just nectar and floral size traits, average bias when ALL QTLs were used (-0.0968) was
433 about half the bias when just GWS QTLs were used (-0.201), a difference that was significant with a
434 bootstrap comparison ($P < 0.001$).

435

436 **Analysis of selection**

437 A strong preponderance of QTLs with RHE in the direction of the species difference (“consistent-directional
438 QTLs”) compared to the opposite direction (“contra-directional QTLs”) is an expected signature of selection.
439 Overall, 81.5% of QTLs were consistent-directional, with the proportion for ALL QTLs being larger than for
440 GSW QTLs (Table S8), a pattern consistent with selection acting on many of the traits examined.

441

442 Both the QTL-EE sign test and the Fraser test support this inference. With the former test, for GWS QTLs,
443 most of the floral traits have a nominally to borderline significant excess of consistent-directional QTLs, with
444 corolla width and corolla length significant at $P < 0.05$ after correcting for multiple comparisons (Table S4A).
445 For ALL QTLs, all floral size and nectar traits, except for sepal length, were found to be nominally
446 significant, with most of the floral size traits and nectar sugar concentration remaining significant after
447 correcting for multiple comparisons (Table S4B). The Fraser ν test statistic is highly significant for all traits (all
448 $P < 0.002$; Table 3), except sepal length and all three seed traits, and remain significant at an overall level of P
449 < 0.01 after a sequential Bonferroni correction. Overall, these results are consistent with selection having
450 acted on all three nectar traits and all floral traits except sepal length, and agree with findings from a previous
451 QstFst analysis (Rifkin *et al.*, 2019b).

452

453 Contra-directional QTLs weaken the ability to detect selection because the alleles fixed are assumed to be due
454 to genetic drift. Alternatively, contra-directional QTLs may have advantageous pleiotropic effects on other
455 characters and were fixed because of those positive effects. Most floral size and nectar contra-directional
456 QTLs overlap with at least one other floral or nectar QTL with consistent-directional effects (Table S9). This
457 observation is consistent with many of the contra-directional QTLs being fixed by selection, which would
458 make the role of selection in the evolution of these traits even stronger than is revealed by the Fraser and
459 QTL-EE sign tests.

460

461 Anderson and Slatkin (2003) demonstrate that ascertainment bias can increase the rate of false positives in the
462 QTL-EE test and likely also for the Fraser test. However, their analyses implemented an extreme version of
463 ascertainment bias, in which the most diverged trait was chosen out of N candidate traits measured. Because
464 we believe this does not reflect how organismal traits are selected for analysis (see Results and Methods S1),
465 we performed simulations that relax this assumption (Results and Methods S1). Briefly, we assume that traits
466 for study are chosen randomly from the βN candidate loci with the highest divergence. β is thus an index of

467 **Table 3 Fraser (2020) test for selection on each trait.**

468 Columns are components of Equation [2] in Fraser (2020), ν statistic given by that equation, and probability of ν being as large or larger than observed
 469 by chance. A t value of 1.0 was used in all calculations (Methods S9). All significant P values remain significant at an overall level of $P < 0.01$ after a
 470 sequential Bonferroni correction for multiple comparisons (indicated by asterisks).

	Between-Species Variance Component	Number of CORD parents	CORD parent variance	Number LAC parents	LAC parent variance	F5 Between-Line variance component	F5 Within-Line variance component	H ² (Broad-sense heritability)	F5 Phenotypic Variance	ν (test statistic)	P (significance of test)
Corolla Width	66.656	25	1.759	26	1.801	2.450	2.261	0.520	4.678	27.339	0.00001526*
Corolla Throat	1.687	25	0.146	26	0.116	0.155	0.137	0.531	0.290	10.895	0.001*
Corolla Length	41.030	25	1.016	26	1.186	1.652	1.849	0.472	3.489	24.867	1.5259E-05*
Overall Corolla Length	74.652	25	1.434	26	1.993	2.515	2.094	0.546	4.583	29.795	1.5259E-05*
Sepal Length	0.203	25	0.243	26	0.490	0.363	0.446	0.449	0.806	0.482	0.490
Longest Stamen Length	23.796	25	0.255	26	0.337	0.911	0.801	0.532	1.692	26.400	1.5259E-05*
Pistil Length	13.970	25	0.686	26	0.545	1.480	0.702	0.678	2.173	9.443	0.002
Seed Mass	0.000	24	0.000	25	0.000	0.000	0.000	0.620	0.000	0.874	0.350
Seed Length	0.090	24	0.034	25	0.033	0.088	0.034	0.724	0.121	0.989	0.320
Seed Width	0.050	24	0.035	25	0.026	0.048	0.034	0.588	0.081	0.992	0.320
Nectar Volume	3.557	25	0.374	26	0.052	0.161	0.242	0.400	0.402	22.016	1.5259E-05*
Nectar Sugar Concentration	9056.500	25	191.533	26	1089.830	602.835	714.065	0.458	1312.340	14.993	0.0001*
Nectary Size	0.008	25	0.001	26	0.000	0.001	0.000	0.565	0.001	12.788	0.0004*

471

472 the intensity of ascertainment bias, with low values indicating high intensity. In Anderson and Slatkin's study,
473 $\beta = 1/N$. We find that to correct for ascertainment bias, the probability value from the test must be
474 multiplied by β to obtain the true probability. Although there is admittedly no theoretical or empirical
475 guidance, we believe it is unrealistic to assume that traits chosen for study are among the top 0.15 or less (see
476 Results and Methods S1 for justification). Thus, we interpret a P value of less than $0.05 \cdot 0.15 = 0.0075$ as
477 strong evidence for selection despite any ascertainment bias. We also believe that it may be unlikely to choose
478 traits from among the top 0.4 most diverged traits, which would mean that a P value of less than $0.05 \cdot 0.4 =$
479 0.02 may be consistent with selection. Based on these criteria, our analyses indicate that, except for corolla
480 throat and pistil length, the signatures of selection we detected on floral size and nectar traits are not likely an
481 artifact of such bias (Results and Methods S1). More generally, our analyses indicate that ascertainment bias
482 likely does not inflate the probability of obtaining false positives in the QTL-EE and Fraser tests nearly as
483 much as suggested by Anderson and Slatkin (2003).

484

485 DISCUSSION

486

487 Nectar Traits and Floral Size Traits are Separate Evolutionary Modules

488 Flowers are complex structures that perform a variety of functions that are affected by floral size and shape,
489 nectar production, and pollen production. Divergence in these traits is common between closely related
490 species due to changes in either the predominant pollinators or favored mating system. Whether this
491 divergence is constrained by pleiotropy and genetic correlations among floral traits is a long-standing question
492 in plant evolutionary biology (Smith, 2016; Wessinger & Hileman, 2016; Kostyun *et al.*, 2019). While some
493 recent studies have attempted to identify the degree of genetic correlations and modularity among floral traits
494 among species (Dellinger *et al.*, 2019; Dellinger, 2020; Reich *et al.*, 2020), we are still largely ignorant of
495 whether flowers consist of distinct evolutionary modules and, if so, what those modules are.

496

497 The flowers of *Ipomoea lacunosa* and *I. cordatotriloba* consist of at least two distinct evolutionary modules: floral
498 size traits and nectar traits. A previous study of these species only examined one nectar trait (nectar volume),
499 which clustered with floral size traits (Rifkin *et al.*, 2021). By including additional nectar traits, we could
500 distinguish these modules by the moderately high within-module genetic correlations, but low between-
501 module correlations (Table 2a). This pattern is also reflected in the degree of QTL overlap, which is on
502 average higher within the two modules than between them. This genetic architecture indicates that the
503 evolution of decreased floral size in *I. lacunosa* has been largely genetically independent of the evolution of
504 reduced nectar production and *vice versa*.

505

506 Limited information exists in other species regarding the genetic and evolutionary independence of floral size
507 and nectar traits. Across multiple species within the same genus, floral size is phylogenetically correlated with
508 nectar volume (Galetto & Bernardello, 2004; Kaczorowski *et al.*, 2005; Tavares *et al.*, 2016), but such patterns
509 are uninformative about evolutionary independence. Within species, artificial selection for floral size in
510 *Eichhornia paniculata* resulted in a correlated response in nectar volume, indicating that size and nectar volume
511 are genetically correlated, but the magnitude of the correlation is unknown (Worley & Barrett, 2000). Genetic
512 correlations between aspects of flower size and nectar production in *Nicotiana glauca* were non-significant
513 (Kaczorowski *et al.*, 2008), consistent with the existence of separate floral size and nectar modules. Despite
514 these two studies, the genetic architecture of within-species variation is not necessarily indicative of the
515 genetic architecture of divergence for two reasons: (1) genetic correlations can change under selection
516 (Sheridan & Barker, 1974; Mitchell-Olds & Rutledge, 1986; Falconer & Mackay, 1996; Roff, 2007; Arnold *et*
517 *al.*, 2008), and (2) new mutations do not necessarily reflect the correlation structure of standing genetic
518 variation.

519
520 A few QTL studies have examined nectar trait divergence between species, but most report only phenotypic
521 correlations between aspects of floral size and only one or two nectar traits. These studies reveal moderate to
522 complete QTL overlap between floral size and nectar volume. For *Petunia integrifolia* and *P. axillaris*, all four
523 nectar volume QTLs overlap with floral size QTLs with the highest phenotypic correlation between the lower
524 subdomain of the corolla tube and nectar volume (0.58; Galliot *et al.*, 2006). For *Ipomopsis guttata* and *I.*
525 *tenuifolia*, two nectar volume QTLs overlap with floral size QTLs (Nakazato *et al.*, 2013). For *Penstemon*
526 *amphorellae* and *P. kunthii*, nectar volume is correlated with lateral stamen length (0.742) and nectary size
527 (0.603; Katzer *et al.*, 2019). Finally, for *Aquilegia brevistyla* and *A. canadensis*, nectar volume and sepal traits had
528 an average phenotypic correlation of 0.53 and an average QTL overlap of 0.4, but nectary size and sepal traits
529 had a higher average correlation (0.673) and QTL overlap (0.53; Edwards *et al.*, 2021). While these findings
530 are not completely in line our results, none of these studies attempt to identify evolutionary modules, nor do
531 they consider the extent to which QTL co-localization reflects actual genetic correlations among traits. It is
532 thus unclear whether the genetic architecture of divergence in these species differs fundamentally from that
533 we report.

534
535 One explanation for the independence of floral size and nectar modules is differences in the developmental
536 timing of these traits. Although the development of the flower and the floral nectary are undoubtedly linked,
537 they may differ in the timing of cell fate specification and the coordination between cell division and
538 expansion. The nectary often develops *after* floral organs have been specified (Smyth *et al.*, 1990; Baum *et al.*,
539 2001; Thornburg, 2007; Jeiter *et al.*, 2017); in these *Ipomoea* species, the nectary is not visibly present in the

540 earliest stages of flower development when the four major floral organs are easily identifiable (personal
541 observation).

542

543 Floral integration may be diminished in selfing species (Anderson & Busch, 2006), although a meta-study
544 suggests otherwise (Fornoni *et al.*, 2016). By examining traits in addition to floral size, our study and a parallel
545 study (Rifkin *et al.*, 2021) support weakening floral integration in selfing species. Rifkin *et al.* (2021)
546 demonstrated that pollen traits (pollen number and pollen size) constitute a distinct evolutionary module.
547 Although neither study address whether pollen and nectar traits constitute distinct modules, they raise the
548 possibility that flowers in these species consist of at least three distinct evolutionary modules.

549

550 **Structure of the Nectar Module**

551 Galetto and Bernadello (2004) report a correlation between nectar volume and nectary size across six *Ipomoea*
552 species. Additionally, within *Nicotiana glauca*, there is a high genetic correlation (0.89) between nectar volume
553 and nectar energy content (total sugar amount) (Kaczorowski *et al.*, 2008). These two findings suggest that (1)
554 physiologically, nectar volume and sugar content are proportional to nectary size and that (2) these three traits
555 may comprise a distinct evolutionary module. If the hypothesis is true, evolutionary changes in nectar volume
556 and sugar content could primarily be correlated responses to changes in nectary size. Although this
557 hypothesis is not supported in the divergence for *Petunia axillaris* and *P. integrifolia*, where nectar volume and
558 nectar sugar concentration differ between the two species but the nectary size remains the same (Stuurman *et al.*
559 *et al.*, 2004), it may be true for other species, such as *Aquilegia brevistyla* and *A. canadensis* (Edwards *et al.*, 2021).

560

561 Our results are somewhat consistent with this hypothesis. Nectar volume and total sugar content are each
562 moderately genetically correlated with nectary size ($r \approx 0.65$ in both cases, Table S2) and highly correlated
563 with each other (Fig. S4). Sugar concentration is also positively genetically correlated with nectary size with r
564 ≈ 0.65 , and both nectar volume and nectar sugar concentration have moderately high QTL overlap with
565 nectary size (0.66 and 0.5, respectively, Table S5). However, with genetic correlations of this magnitude,
566 correlated responses to selection on nectary size would explain less than half of the variation in nectar volume
567 and total sugar. The rest would be accounted for by mutations that affect volume and/or total sugar but not
568 nectary size. Even within the nectar module, there is substantial independent evolution of the component
569 traits.

570

571 **Selection on Floral Size and Nectar Traits**

572 Two previous QstFst studies determined that natural selection contributed to the divergence of five floral size
573 and two nectar traits between *Ipomoea lacunosa* and *I. cordatotriloba* (Duncan & Rausher, 2013b; Rifkin *et al.*,
574 2019b, 2021). However, neither study was able to distinguish between selection acting directly on these

575 characters and indirect selection due to correlations with selected characters. The QTL-EE sign test and the
576 Fraser test presented here also reveal that divergent selection likely operated on both floral size and nectar
577 traits. By combining these results with our information on genetic architecture, we infer that some floral size
578 traits and some nectar traits likely diverged due to direct selection on those traits; the weak genetic
579 correlations between the two modules would unlikely yield detectable signatures of indirect selection. Because
580 of the high within-module genetic correlations, we cannot distinguish between direct and indirect selection
581 for traits within the same module. Moreover, our study is unable to identify the causes of selection acting on
582 these traits, *i.e.* whether selection in *I. lacunosa* was favored by advantages of resource re-allocation, increased
583 rate in floral development, or decreased florivory (Sicard & Lenhard, 2011).

584

585 Ascertainment biases, in the form of choosing to study characters that are known to have diverged between
586 species, can bias both QTL-EE sign tests and the Fraser test, artificially increasing the probability of
587 obtaining false positives (Anderson & Slatkin, 2003). However, we believe that ascertainment biases do not
588 account for the apparent selection on nectar and floral size traits for three reasons. First, our results are
589 consistent with previous selection detected by a completely different method (Duncan & Rausher, 2013b;
590 Rifkin *et al.*, 2019b). Second, nine of ten floral size and nectar traits are highly significant ($P < 0.002$) by the
591 Fraser test (Table 3), and for seven of these traits, neutrality can be rejected if they were chosen for study
592 from more than the top 15% of candidate traits in terms of divergence (Results and Methods S1). Finally, for
593 these seven traits, the maximum number of candidate traits from which each of those traits can be drawn for
594 rejection of neutrality is likely much higher than the actual number of candidate traits. Generally, the results
595 of our analyses of ascertainment bias also indicates that they likely do not inflate the probability of false
596 positives nearly as much as suggested by Anderson and Slatkin.

597

598 **Do QTL Traits Predict the Genetic Architecture of Divergence?**

599 QTL studies often infer properties of the genetic architecture of divergence from patterns of QTL overlap
600 (*e.g.* Slotte *et al.*, 2012; Wessinger *et al.*, 2014; Kostyun *et al.*, 2019). Seldom are these inferences evaluated by
601 comparing the patterns of QTL overlap and the actual genetic correlations among traits. One exception is a
602 meta-study by Gardner and Latta (2007), which used QTL properties from published studies to predict
603 genetic correlations among traits and compared those estimates to actual genetic correlations. Because most
604 of the studies examined quantified patterns of within-species variation, it is unclear whether these patterns
605 can be extended to the genetic architecture of divergence between species.

606

607 Our results indicate that QTL properties can predict genetic architecture reasonably well qualitatively. As in
608 Gardner and Latta (2007), the magnitudes of the observed genetic correlations in our study are positively
609 correlated with QTL overlap and with predicted genetic correlations, with the strength of the correlation

610 being similar to or higher than reported by Gardner and Latta (Fig. 5). This conclusion also extends to the
611 modular nature of divergence: the average QTL overlap within and between modules generally mirrors the
612 average genetic correlations within and between modules.

613

614 Bias, the difference between the predicted and observed genetic correlation, increased as total RHE
615 decreased. Despite the tendency for QTL effects to be overestimated in studies with fewer than 500
616 individuals (Beavis *et al.*, 1994; Xu, 2003), RHE can be interpreted as an index of the completeness of QTL
617 identification. Based on this, our results indicate that the accuracy of the predicted genetic architecture is
618 proportional to the degree to which all QTLs affecting the traits have been identified. In our study, total RHE
619 was generally high for flower size and nectar traits, and the corresponding genetic correlations had little bias.
620 By contrast, total RHE was low for seed traits, and the bias in the predicted correlation was substantial. We
621 conclude that it is dangerous to make inferences about genetic architecture and constraints on evolution
622 based on QTL overlap unless most of the QTLs affecting the traits of interest have been identified. Thus,
623 while QTL studies can confirm the molecular underpinnings of genetic correlations, assessment of the
624 genetic architecture of genetic correlations can be done more reliably by estimating those correlations directly.

625

626 Finally, although QTLs identified as significant only at the chromosome-wide level (CWS) are often
627 considered less reliable than those significant genome-wide, our results indicated that the CWS QTLs we
628 detected are likely real because including these QTLs in our analyses provided improved estimates of the
629 genetic architecture of divergence. If CWS QTLs were artifactual, we would expect (1) correlations to *decrease*,
630 (2) bias to *increase*, and (3) proportion of QTLs in the same direction of the species difference to be 0.5. We
631 do not observe any of these expectations. First, the correlation between the observed genetic correlations (r_G)
632 and QTL overlaps are higher when CWS QTLs are included (Fig. 4); the same is true for the correlation
633 between observed and predicted genetic correlations (r_P) (Fig. 5a,b). Second, bias in the predicted genetic
634 correlations is less when all QTLs are used than when just GWS QTLs are used. Finally, the proportion of
635 CWS QTLs that have effects in the direction of the species difference is similar to that for GWS QTLs and
636 much greater than 0.5 (Table S8).

637

638 **ACKNOWLEDGEMENTS**

639 We would like to thank members of the Rausher lab for feedback and advice on the experimental design,
640 analyses, and manuscript; Fred Nijhout for use of the microscope for imaging nectaries. We would
641 particularly like to thank Wendy Dong, Melissa Baldino, Avery Fulford, and Cristian Tolento and members of
642 the Duke Greenhouse Staff, who all helped with plant care and maintenance. This research was supported in
643 part by NSF grant DEB 1542387.

644

645 **AUTHOR CONTRIBUTION**

646 ITL and MDR designed the project, collected and analyzed the data, and wrote the manuscript. JLR
647 performed final computational analyses for the linkage map and edited the manuscript. GC annotated the
648 draft genome necessary for the randomization test.
649

650 **DATA AVAILABILITY**

651 Raw sequence data from this study are found NCBI Sequence Read Archive [accession: PRJNA732507].
652 Scripts for sequence processing and linkage mapping are openly available on GitHub at
653 https://github.com/joannarifkin/Ipomoea_QTL/. All other scripts are openly available on GitHub at
654 <https://github.com/itliao/IpomoeaNectarQTL>.
655

656 **ORCID**

657 Irene T. Liao: orcid.org/0000-0002-2904-4117
658 Joanna L. Rifkin: orcid.org/0000-0003-1980-5557
659 Gongyuan Cao: orcid.org/0000-0003-4417-251X
660 Mark D. Rausher: orcid.org/0000-0002-6541-9641
661

662 **SUPPORTING INFORMATION**

663 **Fig. S1** Genetic map and distribution of the 6056 markers used for the QTL analysis.
664 **Fig. S2** Cluster diagrams based on covariance-component genetic correlations.
665 **Fig. S3** Frequency distributions of 13 phenotypic traits
666 **Fig. S4** Pairwise correlations and regressions for the three measured nectar traits and total sugar content.
667 **Fig. S5** Comparison of correlations derived from RIL means and from variance-covariance (var-covar)
668 components.
669 **Fig. S6** Pairwise trait correlations among the 13 traits.
670 **Fig. S7** QTL plots for individual traits.
671
672 **Methods S1** Materials and growing conditions and phenotyping nectar traits (nectar volume, nectar sugar
673 concentration, nectary size).
674 **Methods S2** Summary protocol for ddRAD sequencing.
675 **Methods S3** Sequence processing and linkage mapping.
676 **Methods S4** Calculating genetic correlations and broad-sense heritabilities.

677 **Methods S5** Permutation test for cluster analysis.

678 **Methods S6** Randomization test.

679 **Methods S7** Quantifying QTL overlap and permutation test.

680 **Methods S8** Predicting genetic correlations from QTL properties and permutation analysis.

681 **Methods S9** Fraser ν -test statistic.

682

683 **Results and Methods S1** Ascertainment bias analysis and results.

684

685 **Table S1** List of individuals phenotyped but NOT genotyped

686 **Table S2** Genetic correlations derived from variance-covariance components for the 13 phenotypic traits
687 measured.

688 **Table S3** QTL characteristics for all trait QTLs.

689 **Table S4** Summary of aggregate QTL characteristics for individual traits

690 **Table S5** Pairwise QTL overlap.

691 **Table S6** Randomization test (random placement of QTLs in genome) of whether QTLs within modules are
692 spatially clustered in the genome.

693 **Table S7** Average predicted genetic correlations, r_G , within and between modules with standard errors (in
694 parentheses).

695 **Table S8** Number of QTLs with effects in same direction as or opposite direction from difference between
696 species.

697 **Table S9** Contra-directional QTLs summary.

698

699

700

701

702

703

704

705

706

707

708

709

710

711

712 **REFERENCES**

713

- 714 **Anderson IA, Busch JW. 2006.** Relaxed pollinator-mediated selection weakens floral integration in self-
715 compatible taxa of *Leavenworthia* (Brassicaceae). *American Journal of Botany* **93**: 860–867.
- 716 **Anderson EC, Slatkin M. 2003.** Orr’s quantitative trait loci sign test under conditions of trait ascertainment.
717 *Genetics* **165**: 445–446.
- 718 **Armbruster WS, Pelabon C, Bolstad GH, Hansen TF. 2014.** Integrated phenotypes: understanding trait
719 covariation in plants and animals. *Philosophical Transactions of the Royal Society B* **369**: 20130245–20130245.
- 720 **Armbruster WS, Pelabon C, Hensen TF, Mulder CPH. 2004.** Floral integration, Modularity, and
721 Accuracy: Distinguishing Complex Adaptations from Genetic Constraints. In: Pigliucci M, Preston K, eds.
722 Phenotypic Integration: Studying the Ecology and Evolution of Complex Phenotypes. 22–49.
- 723 **Armbruster WS, Stilio VS Di, Tuxill JD, Flores TC, Runk JLV. 1999.** Covariance and Decoupling of
724 Floral and Vegetative Traits in Nine Neotropical Plants: A Re-Evaluation of Berg’s Correlation-Pleiades
725 Concept. *American Journal of Botany* **86**: 39–55.
- 726 **Arnold SJ. 1992.** Constraints on Phenotypic Evolution. *The American Naturalist* **140**: S85–S107.
- 727 **Arnold SJ, Bürger R, Hohenlohe PA, Ajie BC, Jones AG. 2008.** Understanding the evolution and stability
728 of the G-matrix. *Evolution* **62**: 2451–2461.
- 729 **Arunkumar R, Ness RW, Wright SI, Barrett SCH. 2015.** The Evolution of Selfing Is Accompanied by
730 Reduced Efficacy of Selection and Purging of Deleterious Mutations. *Genetics* **199**: 817–829.
- 731 **Ashman T-L, Majetic CJ. 2006.** Genetic constraints on floral evolution: a review and evaluation of patterns.
732 *Heredity* **96**: 343–352.
- 733 **Baldwin BG, Kalisz S, Scott Armbruster W. 2011.** Phylogenetic perspectives on diversification,
734 biogeography, and floral evolution of *Collinsia* and *Tonella* (Plantaginaceae). *American Journal of Botany* **98**: 731–
735 753.
- 736 **Barrett SCH. 2002.** The Evolution of Plant Sexual Diversity. *Nature Reviews Genetics* **3**: 274–284.
- 737 **Baum SF, Eshed Y, Bowman JL. 2001.** The *Arabidopsis* nectary is an ABC-independent floral structure.
738 *Development* **128**: 4657–67.
- 739 **Beavis WD, Smith OS, Grant D, Fincher R. 1994.** Identification of quantitative trait loci using a small
740 sample of topcrossed and F4 progeny from maize. *Crop Science* **34**: 882–896.
- 741 **Benjamini Y, Hochberg Y. 1995.** Controlling the False Discovery Rate : A Practical and Powerful Approach
742 to Multiple Testing. *Journal of the Royal Statistical Society. Series B (Methodological)* **57**: 289–300.
- 743 **Berg RL. 1960.** The Ecological Significance of Correlation Pleiades. *Evolution* **14**: 171–180.
- 744 **Broman KW, Gatti DM, Simecek P, Furlotte NA, Prins P, Sen S, Yandell BS, Churchill GA. 2019.**
745 R/qt2: Software for mapping quantitative trait loci with high-dimensional data and multiparent populations.

- 746 *Genetics* **211**: 495–502.
- 747 **Broman KW, Wu H, Sen S, Churchill GA. 2003.** R/qtl: QTL mapping in experimental crosses.
- 748 *Bioinformatics* **19**: 889–890.
- 749 **Cheverud JM. 1984.** Quantitative genetics and developmental constraints on evolution by selection. *Journal of*
- 750 *Theoretical Biology* **110**: 155–171.
- 751 **Conner JK, Cooper IA, La Rosa RJ, Pérez SG, Royer AM. 2014.** Patterns of phenotypic correlations
- 752 among morphological traits across plants and animals. *Philosophical Transactions of the Royal Society B: Biological*
- 753 *Sciences* **369**.
- 754 **Dellinger AS. 2020.** Pollination syndromes in the 21st century: where do we stand and where may we go?
- 755 *New Phytologist* **228**: 1193–1213.
- 756 **Dellinger AS, Artuso S, Pamperl S, Michelangeli FA, Penneys DS, Fernández-Fernández DM, Alvear**
- 757 **M, Almeda F, Scott Armbruster W, Staeder Y, et al. 2019.** Modularity increases rate of floral evolution and
- 758 adaptive success for functionally specialized pollination systems. *Communications Biology* **2**.
- 759 **Diggle PK. 2014.** Modularity and intra-floral integration in metamerism: Plants are more than the
- 760 sum of their parts. *Philosophical Transactions of the Royal Society B: Biological Sciences* **369**.
- 761 **Duncan TM, Rausher MD. 2013a.** Morphological and genetic differentiation and reproductive isolation
- 762 among closely related taxa in the *Ipomoea* series *Batatas*. *American Journal of Botany* **100**: 2183–2193.
- 763 **Duncan TM, Rausher MD. 2013b.** Evolution of the selfing syndrome in *Ipomoea*. *Frontiers in Plant Science* **4**:
- 764 301.
- 765 **Edwards MB, Choi GPT, Derieg NJ, Min Y, Diana AC, Hodges SA, Mahadevan L, Kramer EM,**
- 766 **Ballerini ES. 2021.** Genetic architecture of floral traits in bee- and hummingbird- pollinated sister species of
- 767 *Aquilegia* (columbine).
- 768 **Falconer DS, Mackay TFC. 1996.** *Introduction to quantitative genetics*. Essex, UK: Longman Group Ltd.
- 769 **Fenster CB, Ritland K. 1994.** Quantitative genetics of mating system divergence in the yellow monkeyflower
- 770 species complex. *Heredity* **73**: 422–435.
- 771 **Fishman L, Beardsley PM, Stathos A, Williams CF, Hill JP. 2015.** The genetic architecture of traits
- 772 associated with the evolution of self-pollination in *Mimulus*. *New Phytologist* **205**: 907–917.
- 773 **Fishman L, Kelly AJ, Willis JH. 2002.** Minor Quantitative Trait Loci Underlie Floral Traits Associated with
- 774 Mating System Divergence in *Mimulus*. *Evolution* **56**: 2138.
- 775 **Fornoni J, Ordano M, Pérez-Ishiwara R, Boege K, Domínguez CA. 2016.** A comparison of floral
- 776 integration between selfing and outcrossing species: A meta-analysis. *Annals of Botany* **117**: 299–306.
- 777 **Frazer LJ, Rifkin J, Maheepala DC, Grant A, Wright S, Kalisz S, Litt A, Spigler R. 2021.** New genomic
- 778 resources and comparative analyses reveal differences in floral gene expression in selfing and outcrossing
- 779 *Collinsia* sister species. *G3 Genes | Genomes | Genetics*.
- 780 **Fujikura U, Jing R, Hanada A, Takebayashi Y, Sakakibara H, Yamaguchi S, Kappel C, Lenhard M.**

- 781 2017. Variation in Splicing Efficiency Underlies Morphological Evolution in *Capsella*. *Developmental Cell*: 1–12.
- 782 **Galetto L, Bernardello G. 2004.** Floral nectaries, nectar production dynamics and chemical composition in
783 six *Ipomoea* species (Convolvulaceae) in relation to pollinators. *Annals of Botany* **94**: 269–280.
- 784 **Galliot C, Hoballah ME, Kuhlemeier C, Stuurman J. 2006.** Genetics of flower size and nectar volume in
785 *Petunia* pollination syndromes. *Planta* **225**: 203–12.
- 786 **Gardner KM, Latta RG. 2007.** Shared quantitative trait loci underlying the genetic correlation between
787 continuous traits. *Molecular Ecology* **16**: 4195–4209.
- 788 **Jeiter J, Hilger HH, Smets EF, Weigend M. 2017.** The relationship between nectaries and floral
789 architecture: A case study in Geraniaceae and Hypseocharitaceae. *Annals of Botany* **120**: 791–803.
- 790 **Juenger T, Pérez-Pérez JM, Bernal S, Micol JL. 2005.** Quantitative trait loci mapping of floral and leaf
791 morphology traits in *Arabidopsis thaliana*: evidence for modular genetic architecture. *Evolution & Development* **7**:
792 259–271.
- 793 **Kaczorowski RL, Gardener MC, Holtsford TP. 2005.** Nectar Traits in *Nicotiana* Section *Alatae*
794 (Solanaceae) in Relation to Floral Traits, Pollinators, and Mating System. *American Journal of Botany* **92**: 1270–
795 1283.
- 796 **Kaczorowski RL, Juenger TE, Holtsford TP. 2008.** Heritability and correlation structure of nectar and
797 floral morphology traits in *Nicotiana glauca*. *Evolution* **62**: 1738–1750.
- 798 **Katzer AM, Wessinger CA, Hileman LC. 2019.** Nectary size is a pollination syndrome trait in *Penstemon*.
799 *New Phytologist*. 0–1.
- 800 **Kostyun JL, Gibson MJS, King CM, Moyle LC. 2019.** A simple genetic architecture and low constraint
801 allow rapid floral evolution in a diverse and recently radiating plant genus. *New Phytologist* **223**: 1009–1022.
- 802 **Lande R, Arnold SJ. 1983.** The Measurement of Selection on Correlated Characters. *Evolution* **37**: 1210–
803 1226.
- 804 **McDonald JA, Hansen DR, McDill JR, Simpson BB. 2011.** A Phylogenetic Assessment of Breeding
805 Systems and Floral Morphology of North American *Ipomoea* (Convolvulaceae). *Journal of the Botanical Research*
806 *Institute of Texas* **5**: 159–177.
- 807 **Mitchell-Olds T, Rutledge J. J. 1986.** Quantitative Genetics in Natural Plant Populations: A Review of the
808 Theory. *The American Naturalist* **127**: 379–402.
- 809 **Müllner D. 2013.** Fastcluster: Fast hierarchical, agglomerative clustering routines for R and Python. *Journal of*
810 *Statistical Software* **53**: 1–18.
- 811 **Muñoz-Rodríguez P, Carruthers T, Wood JRI, Williams BRM, Weitemier K, Kronmiller B, Ellis D,**
812 **Anglin NL, Longway L, Harris SA, et al. 2018.** Reconciling Conflicting Phylogenies in the Origin of Sweet
813 Potato and Dispersal to Polynesia. *Current Biology* **28**: 1246-1256.e12.
- 814 **Nakazato T, Rieseberg LH, Wood TE. 2013.** The genetic basis of speciation in the *Giliopsis* lineage of
815 *Ipomopsis* (Polemoniaceae). *Heredity* **111**: 227–237.

- 816 **Ordano M, Fornoni J, Boege K, Domínguez CA. 2008.** The adaptive value of phenotypic floral
817 integration. *New Phytologist* **179**: 1183–1192.
- 818 **Orr HA. 1998.** Testing natural selection vs. genetic drift in phenotypic evolution using quantitative trait locus
819 data. *Genetics* **149**: 2099–2104.
- 820 **Ostevik KL. 2016.** The ecology and genetics of adaptation and speciation in dune sunflowers.
- 821 **Peterson BK, Weber JN, Kay EH, Fisher HS, Hoekstra HE. 2012.** Double digest RADseq: An
822 inexpensive method for de novo SNP discovery and genotyping in model and non-model species. *PLoS ONE*
823 **7**.
- 824 **Rastas P. 2017.** Lep-MAP3: Robust linkage mapping even for low-coverage whole genome sequencing data.
825 *Bioinformatics* **33**: 3726–3732.
- 826 **Reich D, Berger A, von Balthazar M, Chartier M, Sherafati M, Schönenberger J, Manafzadeh S,**
827 **Staedler YM. 2020.** Modularity and evolution of flower shape: the role of function, development, and
828 spandrels in *Erica*. *New Phytologist* **226**: 267–280.
- 829 **Rifkin JL, Cao G, Rausher MD. 2021.** Genetic Architecture of Divergence : the Selfing Syndrome in
830 *Ipomoea lacunosa*.
- 831 **Rifkin JL, Castillo AS, Liao IT, Rausher MD. 2019a.** Gene flow, divergent selection and resistance to
832 introgression in two species of morning glories (*Ipomoea*). *Molecular Ecology* **28**: 1709–1729.
- 833 **Rifkin JL, Liao IT, Castillo AS, Rausher MD. 2019b.** Multiple aspects of the selfing syndrome of the
834 morning glory *Ipomoea lacunosa* evolved in response to selection: A Qst-Fst comparison. *Ecology and Evolution* **9**:
835 7712–7725.
- 836 **Roff DA. 2007.** A centennial celebration for quantitative genetics. *Evolution* **61**: 1017–1032.
- 837 **Sas C, Müller F, Kappel C, Kent T V., Wright SI, Hilker M, Lenhard M. 2016.** Repeated Inactivation of
838 the First Committed Enzyme Underlies the Loss of Benzaldehyde Emission after the Selfing Transition in
839 *Capsella*. *Current Biology* **26**: 3313–3319.
- 840 **Sedlazeck FJ, Rescheneder P, Von Haeseler A. 2013.** NextGenMap: Fast and accurate read mapping in
841 highly polymorphic genomes. *Bioinformatics* **29**: 2790–2791.
- 842 **Sheridan A, Barker J. 1974.** Two-trait Selection and the Genetic Correlation II. Changes in the Genetic
843 Correlation During Two-trait Selection. *Australian Journal of Biological Sciences* **27**: 89.
- 844 **Sicard A, Lenhard M. 2011.** The selfing syndrome: a model for studying the genetic and evolutionary basis
845 of morphological adaptation in plants. *Annals of Botany* **107**: 1433–1443.
- 846 **Slotte T, Hazzouri KM, Stern D, Andolfatto P, Wright SI. 2012.** Genetic Architecture and Adaptive
847 Significance of the Selfing Syndrome in *Capsella*. *Evolution* **66**: 1360–1374.
- 848 **Smith SD. 2016.** Pleiotropy and the evolution of floral integration. *New Phytologist* **209**: 80–85.
- 849 **Smyth DR, Bowman JL, Meyerowitz EM. 1990.** Early flower development in *Arabidopsis*. *The Plant Cell* **2**:
850 755–767.

851 **Strandh M, Jönsson J, Madjidian JA, Hansson B, Lankinen Å. 2017.** Natural selection acts on floral
852 traits associated with selfing rate among populations of mixed-mating *Collinsia heterophylla* (Plantaginaceae).
853 *International Journal of Plant Sciences* **178**: 594–606.

854 **Stuurman J, Hoballah ME, Broger L, Moore J, Basten C, Kuhlemeier C. 2004.** Dissection of floral
855 pollination syndromes in *Petunia*. *Genetics* **168**: 1585–1599.

856 **Tavares DC, Freitas L, Gaglianone MC. 2016.** Nectar volume is positively correlated with flower size in
857 hummingbird-visited flowers in the Brazilian Atlantic Forest. *Journal of Tropical Ecology* **32**: 335–339.

858 **Team RC.** R: A language and environment for statistical computing.

859 **Thornburg RW. 2007.** Molecular biology of the *Nicotiana* floral nectary. In: Nicolson SW, Nepi M, Pacini M,
860 eds. Nectaries and Nectar. Dordrecht, The Netherlands: Springer, 265–288.

861 **USDA, NRCS. 2021.** The PLANTS Database (<http://plants.sc.egov.usda.gov>, 06/03/2021). National Plant
862 Data Team, Greensboro, NC USA.

863 **Wessinger CA, Hileman LC. 2016.** Accessibility, constraint, and repetition in adaptive floral evolution.
864 *Developmental Biology*: 1–9.

865 **Wessinger CA, Hileman LC, Rausher MD. 2014.** Identification of major quantitative trait loci underlying
866 floral pollination syndrome divergence in *Penstemon*. *Philosophical Transactions of the Royal Society B: Biological*
867 *Sciences* **369**: 20130349–20130349.

868 **Worley AC, Barrett SCH. 2000.** Evolution of Floral Display in *Eichhornia paniculata* (Pontederiaceae): Direct
869 and Correlated Responses to Selection on Flower Size and Number. *Evolution* **54**: 1533–1545.

870 **Wozniak NJ, Kappel C, Marona C, Altschmied L, Neuffer B, Sicard A. 2020.** A Similar Genetic
871 Architecture Underlies the Convergent Evolution of the Selfing Syndrome in *Capsella*. *The Plant Cell*.
872 tpc.00551.2019.

873 **Xu S. 2003.** Theoretical Basis of the Beavis Effect. *Genetics* **165**: 2259–2268.

874 **Yang J, Zaitlen NA, Goddard ME, Visscher PM, Price AL. 2014.** Advantages and pitfalls in the
875 application of mixed-model association methods. *Nature Genetics* **46**: 100–106.

876

877